INTERNATIONAL JOURNAL FOR NUMERICAL AND ANALYTICAL METHODS IN GEOMECHANICS, VOL. 21, 423–441 (1997)

ELASTOPLASTIC RESPONSE OF PRESSURE SENSITIVE SOLIDS

DAVID DURBAN[1] AND PANOS PAPANASTASIOU[2,*]

[1] *Faculty of Aerospace Engineering, Technion, Haifa 32000, Israel*
[2] *Schlumberger Cambridge Research, High Cross, Madingley Road Cambridge CB3 0EL, U.K.*

SUMMARY

Tensorially invariant constitutive relations are systematically derived for large strain elastoplastic response of geomaterials. The analysis centres on Mohr–Coulomb (MC) and Drucker–Prager (DP) models with arbitrary hardening and non-associated response. Both flow and deformation theories are constructed for each model with emphasis on linear incremental relations between the Eulerian strain rate tensor and the objective Jaumann stress rate tensor.

Specifying the results for plane strain compression we find that deformation theory produces a much smaller tangent instantaneous shear modulus than flow theory. It follows that failure of ellipticity and onset of surface instabilities predicted by deformation theory for associated solids occur at much lower levels of strain than the corresponding flow theory results. On the other hand, flow theory predictions admit a considerable sensitivity to the level of non-associativity. In fact, at high levels of non-associativity flow theory predictions for loss of ellipticity can be at strains below those obtained from deformation theory.

Int. J. Numer. Anal. Meth. Geomech., Vol. 21, 423–441 (1997)
(No. of Figures: 8 No. of Tables: 0 No. of Refs: 25)

Key words: Mohr-Coulomb, Drucker-Prager, flow theory, deformation theory, loss of ellipticity, surface instabilities, bifurcation

1. INTRODUCTION

Large strain constitutive modelling of elastoplastic pressure sensitive geomaterials is imperative for the analysis of non-linear behaviour of rocks and soils, especially for discussing possible bifurcations away from the primary equilibrium path.[1–3] The key issue in this context is the instantaneous moduli tensors and their dependence on loading history. Available accounts of elastoplastic response of geomaterials are usually restricted to small strain flow theory versions of the Mohr–Coulomb (MC) and Drucker–Prager (DP) solids (e.g. References 4–6). In metal plasticity, by contrast, it has been recognized long ago that deformation type theories predict bifurcation data[7] which are more realistic than those obtained from flow theories. Plastic buckling—to mention a neighbouring field—is predicted far better with deformation theory[8] because of the low values of instantaneous shear moduli obtained from that model.

* Correspondence to P. Papanastasiou, Schlumberger Cambridge Research, High Cross, Madingley Road, Cambridge CB3 0EL, U.K.

Contract grant sponsor: Technion

CCC 0363–9061/97/070423–19$17.50

Received 29 February 1996
Revised 12 October 1996

This study presents a systematic derivation of large strain MC and DP constitutive relations for both flow and deformation theories. Arbitrary strain hardening is allowed for and plastic response is assumed to be non-associated. Invariant expressions are obtained for incremental constitutive equations that relate the Eulerian strain rate tensor to the objective Jaumann stress rate.

A further specification of the constitutive relations to plane strain deformation patterns enables a comparison of instantaneous moduli for the different material models. Examples are provided for Castlegate sandstone and for Jurassic shale in plane-strain axial compression. It is shown that flow and deformation theories remain in close agreement and that MC predictions (for the primary path) are similar to those of the DP inner cone model. However, the instantaneous shear modulus predicted by deformation theory (in the plastic range) is much smaller than corresponding flow theory modulus (which retains its elastic value G).

It is well known that failure in geomaterials is often accompanied by the concentration of deformation into narrow bands. This observation suggests the construction of failure criteria based on the prediction of the loss of ellipticity and of the emergence of surface instabilities (both events are without a characteristic length). Earlier studies in that direction are, among others.[2,3,9–14] We have calculated, for plane-strain compression, the onset of surface instabilities and failure of ellipticity of the field equations. With the materials investigated (both associated) the main finding is that surface instabilities occur before ellipticity is lost, and that deformation theory predictions (for both events) are at lower levels of strain by comparison with flow theory results. In fact, flow theory predicts surface instabilities and failure of ellipticity at unrealistically high strains. It should be emphasized however that deformation theory is applicable only when the primary loading path is nearly proportional (as in the deformation patterns considered in the present paper). Another shortcoming of deformation theories is that they cannot model elastic unloading which, for example, is likely to occur in the post bifurcation range.

However, a further examination of the influence of non-associativity has revealed that flow theory predictions are sensitive to deviations from associativity; With increasing levels of non-associativity flow theory predicts loss of ellipticity before the onset of surface instabilities. At higher levels of non-associativity flow theory data for failure of ellipticity are at lower strains than those of deformation theory. The latter theory shows little sensitivity to deviations from associativity.

It is conceivable that reliable criteria for failure of rocks should account for appropriate coupling between the occurrence of surface instabilities, possible emergence of localized patterns in non-elliptic fields and level of non-associativity. Of particular interest—inview of the results presented here—is an assessment of the importance of non-normality (deviation from associativity) in making the choice between using flow or deformation theories.

2. MOHR–COULOMB ANALYSIS

Denoting the principal stress components by $(\sigma_1, \sigma_2, \sigma_3)$ and assuming that $\sigma_1 > \sigma_2 > \sigma_3$ we can write the MC effective stress $\bar{\sigma}_e$ and plastic potential $\bar{\phi}$ as

$$\bar{\sigma}_e = \bar{\mu}\sigma_1 - \sigma_3, \qquad \bar{\phi} = \bar{\eta}\sigma_1 - \sigma_3 \tag{1}$$

where $(\bar{\eta}, \bar{\mu})$ are material parameters. Associated behaviour is obtained when $\bar{\eta} = \bar{\mu}$ and the Tresca solid is recovered with $\bar{\eta} = \bar{\mu} = 1$.

The plastic strain rate tensor $\mathbf{D}^{\mathrm{p}}$ is derived within the framework of flow theory from $\bar{\phi}$ via the normality condition

$$\mathbf{D}^{\mathrm{p}} = \Lambda \frac{\mathrm{d}\bar{\phi}}{\mathrm{d}\boldsymbol{\sigma}} \tag{2}$$

where Λ is the proportionality factor and $\boldsymbol{\sigma}$ is the stress tensor. Substituting the plastic potential $\bar{\phi}$ from (1) in (2) poses the question of the derivatives of principal stress components with respect to $\boldsymbol{\sigma}$. To this end we recall the analysis in Durban[15] which shows that

$$\frac{\mathrm{d}\sigma_i}{\mathrm{d}\boldsymbol{\sigma}} = \mathbf{N}_i, \quad i = 1,2,3 \tag{3}$$

where σ_i $(i = 1,2,3)$ are the principal stress components and $\mathbf{N}_i$ $(i = 1,2,3)$ are the associated principal tensors. Thus, the stress tensor can be written as $\boldsymbol{\sigma} = \sigma_i \mathbf{N}_i$ (sum over i) with $\mathbf{N}_i = \mathbf{n}_i \mathbf{n}_i$ (no sum $(i = 1,2,3)$) denoting the diadic product $\mathbf{n}_i \otimes \mathbf{n}_i$, where $\mathbf{n}_i$ are the principal unit vectors associated with $\boldsymbol{\sigma}$. Note, however, that no special symbol is used throughout this report for the diadic (or tensorial) product. It follows that the plastic strain rate tensor (2) is given by

$$\mathbf{D}^{\mathrm{p}} = \Lambda(\bar{\eta}\mathbf{N}_1 - \mathbf{N}_3) \tag{4}$$

Next, we invoke the principle of plastic power equivalence

$$\boldsymbol{\sigma} \cdot \cdot \mathbf{D}^{\mathrm{p}} = \bar{\sigma}_{\mathrm{e}} \dot{\bar{\varepsilon}}_{\mathrm{p}} \tag{5}$$

where $\bar{\varepsilon}_{\mathrm{p}}$ is the total plastic strain and a known function of the effective stress $\bar{\sigma}_{\mathrm{e}}$, and the superposed dot denotes differentiation with respect to a time like parameter. Inserting (4) in (5) we find that

$$\Lambda = \frac{\bar{\sigma}_{\mathrm{e}}}{\bar{\phi}} \dot{\bar{\varepsilon}}_p \tag{6}$$

The time-like derivative $\dot{\bar{\varepsilon}}_{\mathrm{p}}$ can be put in the form

$$\dot{\bar{\varepsilon}}_{\mathrm{p}} = \bar{\varepsilon}'_{\mathrm{p}} \dot{\bar{\sigma}}_{\mathrm{e}} = \bar{\varepsilon}'_{\mathrm{p}} \frac{\mathrm{d}\bar{\sigma}_{\mathrm{e}}}{\mathrm{d}\boldsymbol{\sigma}} \cdot \cdot \dot{\boldsymbol{\sigma}} = \bar{\varepsilon}'_{\mathrm{p}} (\bar{\mu}\mathbf{N}_1 - \mathbf{N}_3) \cdot \cdot \overset{\nabla}{\boldsymbol{\sigma}} \tag{7}$$

where the prime denotes differentiation with respect to $\bar{\sigma}_{\mathrm{e}}$, and $\overset{\nabla}{\boldsymbol{\sigma}}$ is the objective Jaumann stress rate which measures the rate of change of $\boldsymbol{\sigma}$ independently of rigid body rotation. The use of the Jaumann objective stress rate in formulating large strain elastoplastic models is preferable to employing other definitions of objective stress rates; The Jaumann rate $\overset{\nabla}{\boldsymbol{\sigma}}$ behaves in tensorial hyperspaces very similarly to the usual time derivative $\dot{\boldsymbol{\sigma}}$.[16] Combining (6) and (7) with (4) gives the plastic strain rate tensor

$$\mathbf{D}^{\mathrm{p}} = \frac{\bar{\sigma}_{\mathrm{e}} \bar{\varepsilon}'_{\mathrm{p}}}{\bar{\phi}} (\bar{\eta}\mathbf{N}_1 - \mathbf{N}_3)(\bar{\mu}\mathbf{N}_1 - \mathbf{N}_3) \cdot \cdot \overset{\nabla}{\boldsymbol{\sigma}} \tag{8}$$

Assuming that the total strain rate can be decomposed into an elastic Hookean-like part, and a plastic branch given by (8), we arrive at the constitutive relation

$$\mathbf{D} = \mathscr{M} \cdot \cdot \overset{\nabla}{\boldsymbol{\sigma}} \tag{9}$$

where the instantaneous compliance tensor is given by

$$\mathscr{M} = \frac{1}{2G}\left(\mathscr{J} - \frac{v}{1+v}\mathbf{II}\right) + \frac{\bar{\sigma}_e \dot{\bar{\varepsilon}}_p'}{\bar{\phi}}(\bar{\eta}\mathbf{N}_1 - \mathbf{N}_3)(\bar{\mu}\mathbf{N}_1 - \mathbf{N}_3) \tag{10}$$

with $\mathscr{J}$ and $\mathbf{I}$ denoting the fourth and second order unit tensors, respectively. Inverting (9) we obtain

$$\overset{\nabla}{\boldsymbol{\sigma}} = \mathscr{L} \cdot\cdot \mathbf{D} \tag{11}$$

where $\mathscr{L}$ is the tensor of instantaneous moduli given by

$$\begin{aligned}\mathscr{L} = 2G\mathscr{J} + A_1\mathbf{II} - A_2[&v(\bar{\eta}-1)\mathbf{I}(\bar{\mu}\mathbf{N}_1 - \mathbf{N}_3) \\ &+ v(\bar{\mu}-1)(\bar{\eta}\mathbf{N}_1 - \mathbf{N}_3)\mathbf{I} + (1-2v)(\bar{\eta}\mathbf{N}_1 - \mathbf{N}_3)(\bar{\mu}\mathbf{N}_1 - \mathbf{N}_3)]\end{aligned} \tag{12}$$

with

$$A_1 = \frac{1}{\Delta}\left(\frac{v}{1+v}\right)\left[\frac{1}{2G} + (\bar{\mu}\bar{\eta}+1)\frac{\bar{\sigma}_e \dot{\bar{\varepsilon}}_p'}{\bar{\phi}}\right] \tag{13}$$

$$A_2 = \frac{1}{\Delta}\left(\frac{v}{1+v}\right)\frac{\bar{\sigma}_e \dot{\bar{\varepsilon}}_p'}{\bar{\phi}} \tag{14}$$

$$\Delta = \frac{1}{2G}\left[\frac{1-2v}{E} + \left(\frac{1}{1+v}\right)\frac{\bar{\sigma}_e \dot{\bar{\varepsilon}}_p'}{\bar{\phi}}(\bar{\mu}\bar{\eta} + 1 - v(\bar{\mu}+1)(\bar{\eta}+1))\right] \tag{15}$$

(G, E, v) being the usual elastic constants.

It is worth mentioning that the principal tensors $\mathbf{N}_i$ can be expressed in terms of stress invariants; The principal stresses can be written, by a standard theorem, as

$$\begin{Bmatrix}\sigma_1\\ \sigma_2\\ \sigma_3\end{Bmatrix} = \frac{2}{\sqrt{3}}\sqrt{J_2}\begin{Bmatrix}\sin\left(\theta + \frac{2\pi}{3}\right)\\ \sin(\theta)\\ \sin\left(\theta + \frac{4\pi}{3}\right)\end{Bmatrix} + \frac{1}{3}I_1\begin{Bmatrix}1\\1\\1\end{Bmatrix} \tag{16}$$

where θ is given by

$$\sin 3\theta = -\frac{3\sqrt{3}}{2}\frac{J_3}{J_2^{3/2}} \tag{17}$$

in the range $-\pi/6 \leqslant \theta \leqslant \pi/6$. Here we have used the stress invariants

$$I_1 = \mathbf{I} \cdot\cdot \boldsymbol{\sigma}, \qquad J_2 = \frac{1}{2}\mathbf{S} \cdot\cdot \mathbf{S}, \qquad J_3 = \frac{1}{3}(\mathbf{S}\cdot\mathbf{S}) \cdot\cdot \mathbf{S} \tag{18}$$

with $\mathbf{S} = \boldsymbol{\sigma} - \frac{1}{3}\mathbf{II} \cdot\cdot \boldsymbol{\sigma}$ denoting the stress deviator.

Now, the principal tensors that enter the constitutive model (9)–(12) take the simple form

$$\mathbf{N}_1 = \frac{(\boldsymbol{\sigma} - \sigma_2\mathbf{I})\cdot(\boldsymbol{\sigma} - \sigma_3\mathbf{I})}{(\sigma_1 - \sigma_2)(\sigma_1 - \sigma_3)}, \qquad \mathbf{N}_3 = \frac{(\boldsymbol{\sigma} - \sigma_1\mathbf{I})\cdot(\boldsymbol{\sigma} - \sigma_2\mathbf{I})}{(\sigma_3 - \sigma_1)(\sigma_3 - \sigma_2)} \tag{19}$$

along with a similar relation for $\mathbf{N}_2$. Expressions (19) with (16) and (17) enable us to decompose the material moduli tensors $\mathscr{L}$ and $\mathscr{M}$ on any co-ordinate system. It should be noted that existing studies (e.g. Reference 4) arrive at analogous expressions (for small strain plasticity) by inserting the principal stresses from (16) in (1) and (2) and calculating derivatives for the form

$$\frac{\mathrm{d}\sigma_1}{\mathrm{d}\boldsymbol{\sigma}} = \left(\frac{\partial\sigma_1}{\partial J_2}\right)\frac{\mathrm{d}J_2}{\mathrm{d}\boldsymbol{\sigma}} + \left(\frac{\partial\sigma_1}{\partial\theta}\right)\frac{\mathrm{d}\theta}{\mathrm{d}\boldsymbol{\sigma}} + \left(\frac{\partial\sigma_1}{\partial I_1}\right)\frac{\mathrm{d}I_1}{\mathrm{d}\boldsymbol{\sigma}} \tag{20}$$

along with

$$\frac{\mathrm{d}I_1}{\mathrm{d}\boldsymbol{\sigma}} = \mathbf{I}, \qquad \frac{\mathrm{d}J_2}{\mathrm{d}\boldsymbol{\sigma}} = \mathbf{S}, \qquad \frac{\mathrm{d}J_3}{\mathrm{d}\boldsymbol{\sigma}} = \mathbf{S}\cdot\mathbf{S} - \frac{2}{3}J_2\mathbf{I} \tag{21}$$

and

$$\cos(3\theta)\frac{\mathrm{d}\theta}{\mathrm{d}\boldsymbol{\sigma}} = -\frac{\sqrt{3}}{2}J_2^{-5/2}\left[J_2(\mathbf{S}\cdot\mathbf{S} - \tfrac{2}{3}J_2\mathbf{I}) - \tfrac{3}{2}J_3\mathbf{S}\right] \tag{22}$$

Expression (20) is of course identical with (3). On balance the principal axes method appears to be preferable in treating tensorially invariant constitutive relations, particularly for large strains. It is important to mention that this formulation of the MC model is valid only as long as the three principal stresses remain distinct. If the state of stress reaches a vertex then the normality condition (2) is not valid and a different avenue has to be pursued in deriving the constitutive equations.[17] However, it can easily be verified that no such vertex can develop in the numerical examples examined in this paper.

Turning to the MC deformation theory we begin by replacing the plastic strain rates, from (4) and (6), by the finite strain formation

$$\mathbf{E}_L^{\mathrm{p}} = \frac{\bar{\sigma}_{\mathrm{e}}}{\bar{\phi}}\,\bar{\varepsilon}_{\mathrm{p}}(\bar{\eta}\mathbf{N}_1 - \mathbf{N}_3) \tag{23}$$

where $\mathbf{E}_{\mathrm{L}}^{\mathrm{p}}$ is the finite logarithmic plastic strain tensor. Adding the elastic branch and accounting for an initial state of hydrostatic pressure p_0 we get the deformation theory relation

$$\mathbf{E}_{\mathrm{L}} = \frac{1}{2G}\left(\boldsymbol{\sigma} - \frac{\nu}{1+\nu}\mathbf{II}\cdot\cdot\boldsymbol{\sigma}\right) + \frac{\bar{\sigma}_{\mathrm{e}}\bar{\varepsilon}_{\mathrm{p}}}{\bar{\phi}}(\bar{\eta}\mathbf{N}_1 - \mathbf{N}_3) + (1-2\nu)\frac{p_0}{E}\mathbf{I} \tag{24}$$

where $\mathbf{E}_{\mathrm{L}}$ is the finite logarithmic total strain tensor, defined as[8]

$$\mathbf{E}_{\mathrm{L}} = \ln(\mathbf{F}\cdot\mathbf{F}^{\mathrm{T}})^{1/2} \tag{25}$$

$\mathbf{F}$ being the deformation gradient.

The objective rate version of this deformation-type theory is obtained by taking the Jaumann derivative of (24). A few helpful connections in this context are the following:

$$\overset{\nabla}{\mathbf{N}}_1 = \frac{\mathrm{d}\mathbf{N}_1}{\mathrm{d}\boldsymbol{\sigma}} \cdot\cdot \overset{\nabla}{\boldsymbol{\sigma}}, \qquad \overset{\nabla}{\mathbf{N}}_3 = \frac{\mathrm{d}\mathbf{N}_3}{\mathrm{d}\boldsymbol{\sigma}} \cdot\cdot \overset{\nabla}{\boldsymbol{\sigma}} \tag{26}$$

with[15]

$$\frac{\mathrm{d}\mathbf{N}_1}{\mathrm{d}\boldsymbol{\sigma}} = \frac{1}{2}\left(\frac{\mathbf{S}_2\mathbf{S}_2}{\sigma_1 - \sigma_3} + \frac{\mathbf{S}_3\mathbf{S}_3}{\sigma_1 - \sigma_2}\right) \tag{27}$$

$$\frac{\mathrm{d}\mathbf{N}_3}{\mathrm{d}\boldsymbol{\sigma}} = \frac{1}{2}\left(\frac{\mathbf{S}_1\mathbf{S}_1}{\sigma_3 - \sigma_2} + \frac{\mathbf{S}_2\mathbf{S}_2}{\sigma_3 - \sigma_1}\right) \tag{28}$$

where $\mathbf{S}_1, \mathbf{S}_2, \mathbf{S}_3$ are the unit shear tensors

$$\mathbf{S}_1 = \mathbf{n}_2\mathbf{n}_3 + \mathbf{n}_3\mathbf{n}_2, \qquad \mathbf{S}_2 = \mathbf{n}_3\mathbf{n}_1 + \mathbf{n}_1\mathbf{n}_3, \qquad \mathbf{S}_3 = \mathbf{n}_1\mathbf{n}_2 + \mathbf{n}_2\mathbf{n}_1 \tag{29}$$

Also,

$$\dot{\sigma}_1 = \frac{\mathrm{d}\sigma_1}{\mathrm{d}\boldsymbol{\sigma}} \cdot\cdot \overset{\nabla}{\boldsymbol{\sigma}} = \mathbf{N}_1 \cdot\cdot \overset{\nabla}{\boldsymbol{\sigma}}, \qquad \dot{\sigma}_3 = \mathbf{N}_3 \cdot\cdot \overset{\nabla}{\boldsymbol{\sigma}} \tag{30}$$

The objective Jaumann derivative of (24) follows in the form

$$\begin{aligned}\overset{\nabla}{\mathbf{E}}_{\mathrm{L}} = {} & \frac{1}{2G}\left(\overset{\nabla}{\boldsymbol{\sigma}} - \frac{v}{1+v}\,\mathbf{II} \cdot\cdot \overset{\nabla}{\boldsymbol{\sigma}}\right) + \frac{\bar{\sigma}_{\mathrm{e}}\bar{\varepsilon}_{\mathrm{p}}}{\bar{\phi}}\left(\bar{\eta}\,\frac{\mathrm{d}\mathbf{N}_1}{\mathrm{d}\boldsymbol{\sigma}} - \frac{\mathrm{d}\mathbf{N}_3}{\mathrm{d}\boldsymbol{\sigma}}\right) \cdot\cdot \overset{\nabla}{\boldsymbol{\sigma}} \\ & + \frac{(\bar{\sigma}_{\mathrm{e}}\bar{\varepsilon}_{\mathrm{p}})'}{\bar{\phi}}\,(\bar{\eta}\mathbf{N}_1 - \mathbf{N}_3)(\bar{\mu}\mathbf{N}_1 - \mathbf{N}_3) \cdot\cdot \overset{\nabla}{\boldsymbol{\sigma}} + \frac{\bar{\sigma}_{\mathrm{e}}\bar{\varepsilon}_{\mathrm{p}}}{\bar{\phi}^2}\,(\bar{\eta}\mathbf{N}_1 - \mathbf{N}_3)(\bar{\eta}\mathbf{N}_1 - \mathbf{N}_3) \cdot\cdot \overset{\nabla}{\boldsymbol{\sigma}}\end{aligned} \tag{31}$$

where $\overset{\nabla}{\mathbf{E}}_{\mathrm{L}}$ is related to the Eulerian strain rate $\mathbf{D}$ by[19,20]

$$\overset{\nabla}{\mathbf{E}}_{\mathrm{L}} = \mathbf{D} + \left(\frac{1}{2}\right)\left(\frac{a_j^2 + a_k^2}{a_j^2 - a_k^2}\ln\frac{a_j}{a_k} - 1\right)\mathbf{S}_i\mathbf{S}_i \cdot\cdot \mathbf{D} \tag{32}$$

(sum over i with (j, k) taking the cyclic values). Here a_i are the principal stretches. Just to give an example, in direction $\widehat{11}$ we have $\overset{\nabla}{\mathbf{E}}_{\mathrm{L}11} = D_{11}$; while in direction $\widehat{12}$ the strain rate becomes

$$\overset{\nabla}{\mathbf{E}}_{\mathrm{L}12} = \frac{a_1^2 + a_2^2}{a_1^2 - a_2^2}\left(\ln\frac{a_1}{a_2}\right)D_{12} \tag{33}$$

The compliance tensor and the instantaneous moduli tensor can easily be deduced from (31) and rewritten in terms of the stress invariants.

3. DRUCKER–PRAGER MODELS

This model is based on effective stress σ_{e} and plastic potential ϕ defined as

$$\sigma_{\mathrm{e}} = Q + \tfrac{1}{3}\mu I_1, \qquad \phi = Q + \tfrac{1}{3}\eta I_1 \tag{34}$$

where $Q = (\frac{3}{2}\mathbf{S}\cdot\mathbf{S})^{1/2}$ is the von Mises effective stress and (μ, η) are material parameters that reflect the pressure sensitivity of the solid. Associated behaviour is obtained when $\eta = \mu$ and the von Mises material is described by $\eta = \mu = 0$.

Normality and plastic power equivalence, together with the usual elasto-plastic decomposition of the strain rate tensor, lead[21] to the DP flow theory relation $\mathbf{D} = \mathscr{M}\cdot\cdot\overset{\nabla}{\boldsymbol{\sigma}}$ with the compliance tensor

$$\mathscr{M} = \frac{1}{2G}\left(\mathscr{I} - \frac{v}{1+v}\mathbf{II}\right) + \frac{\sigma_e}{\phi}\varepsilon_p'\left(\frac{3\mathbf{S}}{2Q} + \frac{1}{3}\eta\mathbf{I}\right)\left(\frac{3\mathbf{S}}{2Q} + \frac{1}{3}\mu\mathbf{I}\right) \tag{35}$$

Note that here the prime denotes differentiation with respect to the von Mises effective stress σ_e. Inverting (35) and writing $\overset{\nabla}{\boldsymbol{\sigma}} = \mathscr{L}\cdot\cdot\overset{\nabla}{D}$ we find the instantaneous moduli tensor

$$\mathscr{L} = 2G\mathscr{I} + \left(\frac{v}{1+v}\right)\left(\frac{1}{2G\Delta}\right)\left[\mathbf{II} + 3G\frac{\sigma_e}{\phi}\varepsilon_p'\left(\mathbf{II} + \frac{3\mathbf{SS}}{\frac{2}{3}Q^2}\right)\right] - \frac{\sigma_e\varepsilon_p'}{\phi\Delta}\left(\frac{3\mathbf{S}}{2Q} + \frac{1}{3}\eta\mathbf{I}\right)\left(\frac{3\mathbf{S}}{2Q} + \frac{1}{3}\mu\mathbf{I}\right) \tag{36}$$

where

$$\Delta = \frac{1}{2G}\left[\frac{1-2v}{E} + \frac{\sigma_e\varepsilon_p'}{\phi}\left(\frac{\mu\eta}{3} + \frac{3(1-2v)}{2(1+v)}\right)\right] \tag{37}$$

Relations (35)–(37) are essentially identical with those given by Rudnicki and Rice.[1]

The DP deformation theory model is expressed by the constitutive equation[21]

$$\mathbf{E}_L = \frac{1}{2G}\left(\boldsymbol{\sigma} - \frac{v}{1+v}\mathbf{II}\cdot\cdot\boldsymbol{\sigma}\right) + \frac{\sigma_e\varepsilon_p}{\phi}\left(\frac{3\mathbf{S}}{2Q} + \frac{1}{3}\eta\mathbf{I}\right) + (1-2v)\frac{p_0}{E}\mathbf{I} \tag{38}$$

Taking the Jaumann derivative of (38) we obtain its objective rate form. A few useful relations in that context are the derivatives

$$\frac{dQ}{d\boldsymbol{\sigma}} = \frac{3\mathbf{S}}{2Q}, \qquad \frac{d\sigma_e}{d\boldsymbol{\sigma}} = \frac{3\mathbf{S}}{2Q} + \frac{1}{3}\mu\mathbf{I}, \qquad \frac{d\phi}{d\boldsymbol{\sigma}} = \frac{3\mathbf{S}}{2Q} + \frac{1}{3}\eta\mathbf{I} \tag{39}$$

along with $\dot{F} = (dF/d\boldsymbol{\sigma})\cdot\cdot\overset{\nabla}{\boldsymbol{\sigma}}$ for any isotropic scalar function $F(\boldsymbol{\sigma})$. The rate form of (38) follows as

$$\begin{aligned}\overset{\nabla}{\mathbf{E}}_L = {} & \frac{1}{2G}\left(\overset{\nabla}{\boldsymbol{\sigma}} - \frac{v}{1+v}\mathbf{II}\cdot\cdot\overset{\nabla}{\boldsymbol{\sigma}}\right) + \frac{\sigma_e\varepsilon_p}{\phi}\left(\frac{3\overset{\nabla}{\mathbf{S}}}{2Q} - \frac{9\mathbf{SS}}{4Q^3}\cdot\cdot\overset{\nabla}{\boldsymbol{\sigma}}\right) \\ & + \frac{(\sigma_e\varepsilon_p)'}{\phi}\left(\frac{3\mathbf{S}}{2Q} + \frac{1}{3}\eta\mathbf{I}\right)\left(\frac{3\mathbf{S}}{2Q} + \frac{1}{3}\mu\mathbf{I}\right)\cdot\cdot\overset{\nabla}{\boldsymbol{\sigma}} \\ & - \frac{\sigma_e\varepsilon_p}{\phi^2}\left(\frac{3\mathbf{S}}{2Q} + \frac{1}{3}\eta\mathbf{I}\right)\left(\frac{3\mathbf{S}}{2Q} + \frac{1}{3}\eta\mathbf{I}\right)\cdot\cdot\overset{\nabla}{\boldsymbol{\sigma}}\end{aligned} \tag{40}$$

where $\overset{\nabla}{\mathbf{E}}_L$ is related to $\mathbf{D}$ by (32). The inverted form of (40) reads

$$\left(1 + \frac{3G\sigma_e\varepsilon_p}{\phi Q}\right)\overset{\nabla}{\boldsymbol{\sigma}} = 2G\overset{\nabla}{\mathbf{E}}_L + A_1\mathbf{II}\cdot\cdot\overset{\nabla}{\mathbf{E}}_L + A_2\mathbf{SS}\cdot\cdot\overset{\nabla}{\mathbf{E}}_L - A_3(\eta A\mathbf{IS} + B\mathbf{SI})\cdot\cdot\overset{\nabla}{\mathbf{E}}_L \tag{41}$$

where

$$A_1 = \frac{1}{\Delta}\left[\left(\frac{1}{2G} + \frac{3}{2}A\right)\left(\frac{v}{1+v} + \frac{G\sigma_e\varepsilon_p}{\phi Q}\right) - \frac{\eta}{9}B\right] \tag{42}$$

$$A_2 = \left(\frac{1}{1+v}\right)\left(\frac{1}{\Delta}\right)\left(\frac{9}{4Q^2}\right)\left[\left(1 - 2v + \frac{1}{3}\eta EB\right)\frac{\sigma_e\varepsilon_p}{\phi Q} - (1-2v)A\right] \tag{43}$$

$$A_3 = \left(\frac{1}{\Delta}\right)\left(\frac{1}{2Q}\right)\left(1 + \frac{3G\sigma_e\varepsilon_p}{\phi Q}\right) \tag{44}$$

with

$$\Delta = \frac{1}{2G}\left[\frac{1-2v}{E} + \frac{1}{3}\eta B + \frac{3(1-2v)}{2(1+v)}A\right] \tag{45}$$

$$A = \frac{(\sigma_e\varepsilon_p)'}{\phi} - \frac{\sigma_e\varepsilon_p}{\phi^2} \tag{46}$$

$$B = \mu\frac{(\sigma_e\varepsilon_p)'}{\phi} - \eta\frac{\sigma_e\varepsilon_p}{\phi^2} \tag{47}$$

The compliance and instantaneous moduli tensors can be determined with no difficulty from (40) and (41).

4. PLANE STRAIN ANALYSIS

Consider a rectangular block which is uniformly compressed by the stress field ($\sigma_{xx} = \sigma_1$, $\sigma_{yy} = \sigma_3$, $\sigma_{zz} = \sigma_2$) under plane strain conditions (i.e. with no displacement or gradients in the z direction). Non-uniform incremental response of the block is governed by the plane-strain constitutive relations[3]

$$2G^*(D_{xx} - D_{yy}) = (\overset{\nabla}{\sigma}_{xx} - \overset{\nabla}{\sigma}_{yy}) + \delta(\overset{\nabla}{\sigma}_{xx} + \overset{\nabla}{\sigma}_{yy}) \tag{48}$$

$$2G^*\kappa(D_{xx} + D_{yy}) = \alpha(\overset{\nabla}{\sigma}_{xx} - \overset{\nabla}{\sigma}_{yy}) + (\overset{\nabla}{\sigma}_{xx} + \overset{\nabla}{\sigma}_{yy}) \tag{49}$$

$$2G_tD_{xy} = \overset{\nabla}{\sigma}_{xy} \tag{50}$$

where (D_{xx}, D_{yy}, D_{xy}) and $(\sigma_{xx}, \sigma_{yy}, \sigma_{xy})$ are the plane components of $\mathbf{D}$ and $\boldsymbol{\sigma}$, respectively, (G^*, G_t) are instantaneous shear moduli, and (δ, κ, α) are material coupling parameters. The Cartesian (x, y, z) system is here parallel to the faces of the block.

Specifying the MC and DP flow and deformation constitutive relations for the plane-strain deformation pattern we arrive at the following expressions for material moduli and parameters:

(a) *Mohr–Coulomb flow theory* (11) *and* (12)

$$\alpha = \frac{\frac{1}{2}(\bar{\mu}+1)(\bar{\eta}-1)A_2}{2G - (\frac{1}{2}-v)(\bar{\mu}+1)(\bar{\eta}+1)A_2} \tag{51}$$

$$\kappa = \frac{2G + 2A_1 - (\frac{1}{2} + v)(\bar{\mu} - 1)(\bar{\eta} - 1)A_2}{2G - (\frac{1}{2} - v)(\bar{\mu} + 1)(\bar{\eta} + 1)A_2} \tag{52}$$

$$\delta = \frac{\frac{1}{2}(\bar{\mu} - 1)(\bar{\eta} + 1)A_2}{2G + 2A_1 - (\frac{1}{2} - v)(\bar{\mu} - 1)(\bar{\eta} - 1)A_2} \tag{53}$$

$$2G^* = (1 - \alpha\delta)\left[2G - \left(\frac{1}{2} - v\right)(\bar{\mu} + 1)(\bar{\eta} + 1)A_2\right] \tag{54}$$

$$G_t = G \tag{55}$$

where (A_1, A_2) are given by (13) and (14).

(b) *Mohr–Coulomb deformation theory* (31)

$$\alpha = (\bar{\eta} - 1)\left[(\bar{\mu} + 1)\frac{(\bar{\sigma}_e\bar{\varepsilon}_p)'}{\bar{\phi}} + (\bar{\eta} + 1)\frac{\bar{\sigma}_e\bar{\varepsilon}_p}{\bar{\phi}^2}\right]\kappa G^* \tag{56}$$

$$\frac{1}{\kappa} = \left\{\frac{2(1 - 2v)}{2G} + (\bar{\eta} - 1)\left[(\bar{\mu} - 1)\frac{(\bar{\sigma}_e\bar{\varepsilon}_p)'}{\bar{\phi}} + (\bar{\eta} - 1)\frac{\bar{\sigma}_e\bar{\varepsilon}_p}{\bar{\phi}^2}\right]\right\} G^* \tag{57}$$

$$\delta = (\bar{\eta} + 1)\left[(\bar{\mu} - 1)\frac{(\bar{\sigma}_e\bar{\varepsilon}_p)'}{\bar{\phi}} + (\bar{\eta} - 1)\frac{\bar{\sigma}_e\bar{\varepsilon}_p}{\bar{\phi}^2}\right] G^* \tag{58}$$

$$\frac{1}{G^*} = \frac{1}{G} + (\bar{\eta} + 1)\left[(\bar{\mu} + 1)\frac{(\bar{\sigma}_e\bar{\varepsilon}_p)'}{\bar{\phi}} + (\bar{\eta} + 1)\frac{\bar{\sigma}_e\bar{\varepsilon}_p}{\bar{\phi}^2}\right] \tag{59}$$

$$2G_t = \frac{[(a_x^2 + a_y^2)/(a_x^2 - a_y^2)]\ln a_x/a_y}{1/2G + (\bar{\eta} + 1)(\bar{\sigma}_e\bar{\varepsilon}_p)/[(\sigma_{xx} - \sigma_{yy})\bar{\phi}]} \tag{60}$$

Here we need to know the principal stretches (a_x, a_y) along the loading path. These can easily be evaluated from (24), with the aid of the plane strain constant $a_z = 1$, resulting in

$$\ln a_x = \left(\frac{1 + v}{E}\right)[(1 - v)\sigma_{xx} - v\sigma_{yy} + (1 - 2v)p_0] + \bar{\eta}\frac{\bar{\sigma}_e\bar{\varepsilon}_p}{\bar{\phi}} \tag{61}$$

$$\ln a_y = \left(\frac{1 + v}{E}\right)[(1 - v)\sigma_{yy} - v\sigma_{xx} + (1 - 2v)p_0] - \frac{\bar{\sigma}_e\bar{\varepsilon}_p}{\bar{\phi}} \tag{62}$$

where $\bar{\sigma}_e = \bar{\mu}\sigma_{xx} - \sigma_{yy}$ and $\bar{\phi} = \bar{\eta}\sigma_{xx} - \sigma_{yy}$

(c) *Drucker–Prager flow theory* (35) *and* (36)

$$\alpha = \frac{\eta + \beta P_1}{1 - \beta\Gamma P_2^2}\Gamma P_2 \tag{63}$$

$$\kappa = \frac{z}{1 - \beta\Gamma P_2^2} \tag{64}$$

$$\delta = \frac{\mu + \beta P_1}{z}\,\Gamma P_2 \tag{65}$$

$$G^* = G(1 - \beta\Gamma P_2^2)(1 - \alpha\delta) \tag{66}$$

$$G_t = G \tag{67}$$

where

$$\beta = \frac{9(1 - 2\nu)}{2(1 + \nu)} \qquad P_1 = \frac{S_{xx} + S_{yy}}{2Q} \qquad P_2 = \frac{S_{xx} - S_{yy}}{2Q} \tag{68}$$

$$2G\Gamma = \frac{\sigma_e \dot{\varepsilon}_p'}{\phi\Delta} \tag{69}$$

with Δ given by (37), (S_{xx}, S_{yy}) are deviatoric components, and

$$z = 1 + \left(\frac{\nu}{1 + \nu}\right)\left(2\Theta + 3\Gamma + \frac{27}{2}\,\Gamma P_1^2\right) - \frac{1}{2}\,\Gamma\left(\frac{2}{3}\,\eta + 3P_1\right)\left(\frac{2}{3}\,\mu + 3P_1\right) \tag{70}$$

with

$$2G\Theta = \frac{1}{2G\Delta} \tag{71}$$

(d) *Drucker–Prager deformation theory* (40) *and* (41)

$$\alpha = \frac{C_3(S_{xx} - S_{yy}) - \frac{1}{2}C_2(S_{xx}^2 - S_{yy}^2)}{C_0 + \frac{1}{2}C_2(S_{xx} - S_{yy})^2} \tag{72}$$

$$\kappa = \frac{C_0 + 2C_1 - (C_3 + C_4)(S_{xx} + S_{yy}) + \frac{1}{2}C_2(S_{xx} + S_{yy})^2}{C_0 + \frac{1}{2}C_2(S_{xx} - S_{yy})^2} \tag{73}$$

$$\delta = \frac{C_4(S_{xx} - S_{yy}) - \frac{1}{2}C_2(S_{xx}^2 - S_{yy}^2)}{C_0 + 2C_1 - (C_3 + C_4)(S_{xx} + S_{yy}) + \frac{1}{2}C_2(S_{xx} + S_{yy})^2} \tag{74}$$

$$2G^* = (1 - \alpha\delta)\left[C_0 + \frac{1}{2}\,C_2(S_{xx} - S_{yy})^2\right] \tag{75}$$

$$2G_t = C_0\left(\frac{a_x^2 + a_y^2}{a_x^2 - a_y^2}\right)\ln\frac{a_x}{a_y} \tag{76}$$

where

$$\left(1 + \frac{3G\sigma_e\dot{\varepsilon}_p}{\phi G}\right)(C_0, C_1, C_2, C_3, C_4) = (2G, A_1, A_2, \eta A A_3, B A_3) \tag{77}$$

with (A_1, A_2, A_3, A, B) defined in (42)–(47).

It should be noted that in order to determine the primary equilibrium path, the stresses and strains have to be calculated along the deformation history, with due account of the plane strain constraint.

5. NUMERICAL EXAMPLES AND DISCUSSION

Typical plane-strain behaviour in uniaxial compression ($\sigma_{xx} = \sigma_1 = 0$) of two pressure sensitive solids is shown in Figure 1 for flow theories predictions, and in Figure 2 for deformation theories predictions. Both materials, Castlegate sandstones (ss) and Jurassic shale (sh), were modelled by the MC stress–strain characteristic

$$\bar{\varepsilon}_p = \bar{K}(\bar{\sigma}_e - \bar{Y})^n, \quad \bar{\sigma}_e \geqslant \bar{Y} \tag{78}$$

where $\bar{Y}$ denotes the initial yield stress and $(\bar{K}, n)$ are material constants. The experimental data of triaxial compression tests and the fitted curves can be found in Papanastasiou and Durban.[22] The specific values of material parameters used in the calculations are the following:

Castlegate sandstone:

$$E = 8100 \text{ MPa}, \quad \bar{Y} = 25 \text{ MPa}, \quad \bar{\mu} = \bar{\eta} = 3{\cdot}329$$
$$v = 0{\cdot}35, \quad \bar{K} = 9{\cdot}589 \times 10^{-8}, \quad n = 3{\cdot}547$$

Jurassic shale:

$$E = 3700 \text{ MPa}, \quad \bar{Y} = 15 \text{ MPa}, \quad \bar{\mu} = \bar{\eta} = 1{\cdot}826$$
$$v = 0{\cdot}35, \quad \bar{K} = 6{\cdot}278 \times 10^{-7}, \quad n = 2{\cdot}857$$

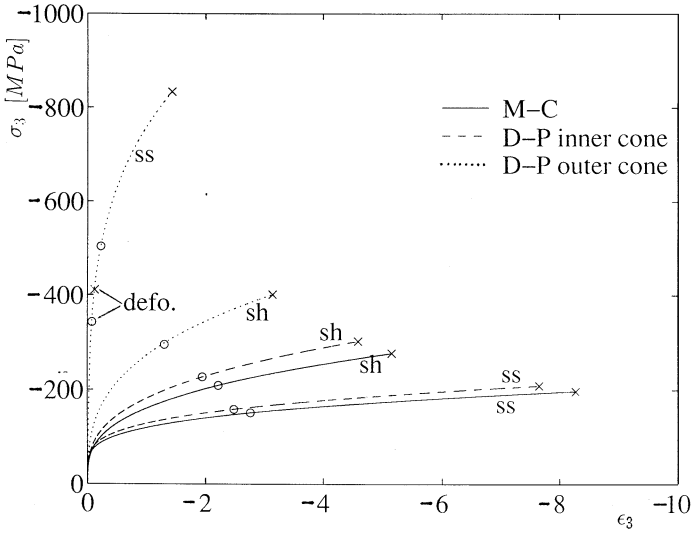

Figure 1. Flow theory stress–strain response in plane-strain axial-compression, for two materials, predicted by different constitutive models, σ_3 is the true axial stress and ε_3 is the true (logarithmic) axial strain. ss—Castlegate sandstone, sh—Jurassic shale. Onset of surface instabilities is indicated by (*o*), loss of ellipticity is indicated by (*x*). Deformation theory predictions for the shale with DP outer cone model are labelled 'defo'

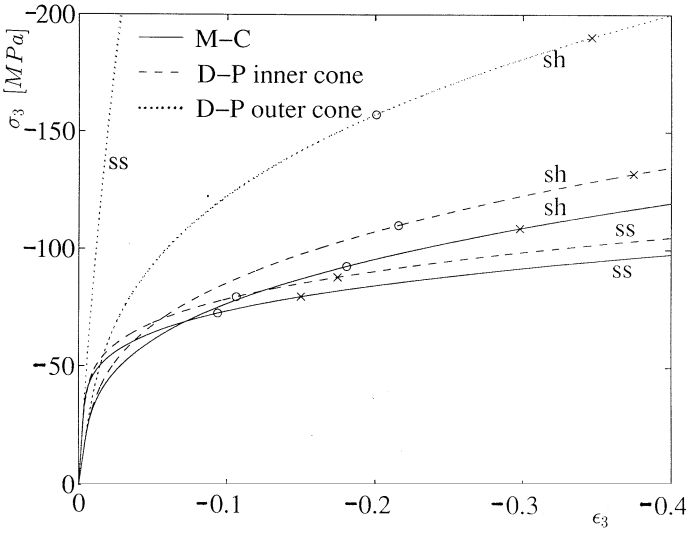

Figure 2. Deformation theory stress–strain response in plane-strain axial-compression, for two materials, predicted by different constitutive models. σ_3 is the true axial stress and ε_3 is the true (logarithmic) axial strain. ss—Castlegate sandstone, sh—Jurassic shale. Onset of surface instabilities is indicated by (o), loss of ellipticity is indicated by (x)

Note that $\bar{K}$ has of (stress)$^{-n}$ and the platic response is associated. That data have been obtained from triaxial compression tests and can be adapted to the analogous DP response function:

$$\varepsilon_{\mathrm{p}} = K(\sigma_{\mathrm{e}} - Y)^n, \quad \sigma_{\mathrm{e}} \geqslant Y \tag{79}$$

where Y is the DP initial yield stress. According to the 'inner cone' and the 'outer cone' DP models there are simple relations between the respective material parameters.[22] If the DP cones (of plastic potential and yield surface) are made to coincide, in the principal stress space, with the generators of the inner apices of the MC hexagonal pyramid then

$$K = \left(\frac{2\bar{\mu}+1}{3}\right)^{n+1}\bar{K}, \qquad Y = \frac{3}{2\bar{\mu}+1}\,\bar{Y}, \qquad \mu = \frac{3(\bar{\mu}-1)}{2\bar{\mu}+1}, \qquad \eta = \frac{3(\bar{\eta}-1)}{2\bar{\eta}+1} \tag{80}$$

Similarly, if the DP cones coincide with the generators of the outer apices of the MC pyramid then

$$K = \left(\frac{\bar{\mu}+2}{3}\right)^{n+1}\bar{K}, \qquad Y = \frac{3}{\bar{\mu}+2}\,\bar{Y}, \qquad \mu = \frac{3(\bar{\mu}-1)}{\bar{\mu}+2}, \qquad \eta = \frac{3(\bar{\eta}-1)}{\bar{\eta}+2} \tag{81}$$

The corresponding constants for the DP models follow as

Castlegate sandstone:

$$\text{inner cone: } K = 6{\cdot}798 \times 10^{-6}, \quad Y = 9{\cdot}80\ \text{MPa}, \quad \mu = \eta = 0{\cdot}912$$

$$\text{outer cone: } K = 1{\cdot}307 \times 10^{-6}, \quad Y = 14{\cdot}07\ \text{MPa}, \quad \mu = \eta = 1{\cdot}311$$

Jurassic shale:

$$\text{inner cone: } K = 3{\cdot}409 \times 10^{-6}, \quad Y = 9{\cdot}67 \text{ MPa}, \quad \mu = \eta = 0{\cdot}533$$

$$\text{outer cone: } K = 1{\cdot}604 \times 10^{-6}, \quad Y = 11{\cdot}76 \text{ MPa}, \quad \mu = \eta = 0{\cdot}648$$

The elastic constants (E, ν) and the hardening exponent n remaining unchanged.

It can be seen from Figures 1 and 2 that the stress–strain response predicted by DP inner cone models and by the MC models remain in fairly close agreement, with a stiffer behaviour predicted by the DP inner cone models. By contrast, the DP outer cone constitutive relations result in considerable deviation from the loading paths obtained from the other models, particularly for the Castlegate sandstone. Notice that the strain and stress scales for the flow theories response (Figure 1) are extended in comparison with deformation theories curves (Figure 2). The reason for this—as it will be shown shortly—is that the flow theories predict loss of ellipticity and occurrence of surface instabilities at much higher levels of strain than those obtained with deformation theory.

It is instructive to compare the instantaneous moduli in plane-strain axial compression ($\sigma_{xx} = \sigma_1 = 0$, $\sigma_{yy} = \sigma_3$). Figure 3 and 4 display the variation of shear moduli (G^*, G_t) and axial tangent modulus $E_t = \mathring{\bar{\sigma}}_{yy}/D_{yy}$ with applied axial compression, for Castegate sandstone. Since that solid is associated both flow and deformation versions of the MC model have exactly the same moduli G^* and E_t with $\bar{\sigma}_e = -\sigma_3$. It can also be seen (Fig. 4) that for the DP model flow and deformation theories predict almost identical results for moduli (G^*, E_t). However, dependence of the tangent shear modulus G_t on applied stress varies considerably between the two theories. While the flow theories predict, by (55) and (67), the constant elastic value $G_t = G$, there is a sharp

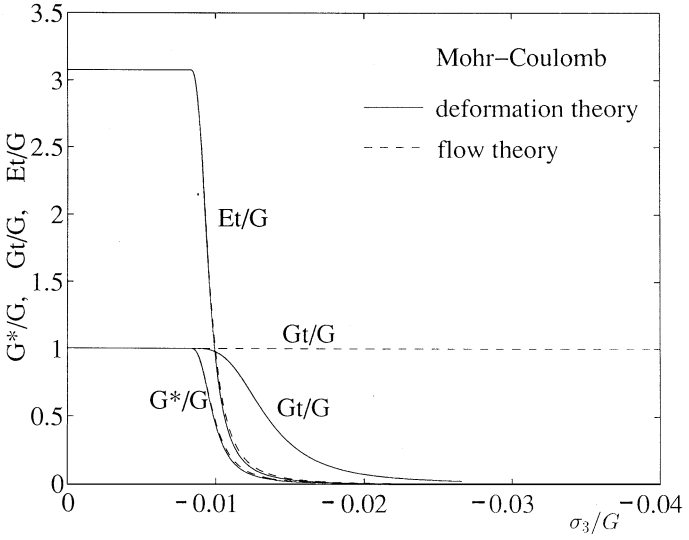

Figure 3. Variation of instantaneous moduli with axial stress in plane-strain compression for Castlegate sandstone according to Mohr–Coulomb models

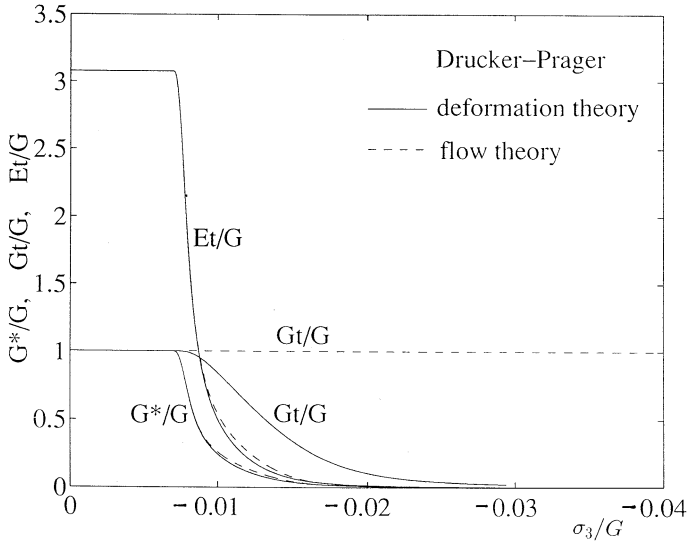

Figure 4. Variation of instantaneous moduli with axial stress in plane-strain compression for Castlegate sandstone according to Drucker–Prager inner cone models

decrease in G_t according to deformation theories, (60) and (76), in the post yield range (Figures 3 and 4). Recent experimental data by Olsson[23] on Tennessee marble appears to corroborate this behaviour of the tangent shear modulus with increasing plastification. For the MC model we find from (60) that in the small strain plastic zone the deformation theory tangent shear modulus is given essentially by

$$G_t \approx \frac{\bar{\sigma}_e}{2(\bar{\mu}+1)\bar{\varepsilon}_p} \tag{82}$$

Since incremental response is governed by the instantaneous moduli, we may expect that the deformation theories will predict a softer behaviour in shear dominated bifurcations away from the primary homogeneous path. To this end we have examined two possible events along the loading history; failure of ellipticity of the governing perturbed field equations and the onset of (short wavelength) surface instabilities. Following the formulation by Chau and Rudnicki[3] we have the condition for loss of ellipticity at the breakdown of the inequality

$$2\frac{G^*}{G_t} > (1+\delta s) - \frac{1}{\kappa}(1+\alpha s) - \left\{(1-s^2)\left[\left(1+\frac{1}{\kappa}\right)^2 - \left(\delta+\frac{\alpha}{\kappa}\right)^2\right]\right\}^{1/2} \tag{83}$$

where

$$s = \frac{\sigma_{xx}-\sigma_{yy}}{2G_t}$$

Similarly, onset of surface instabilities is determined by[3]

$$\frac{A^{1/2}}{C}[PC - Q(R-2B)] + (AQ+PR) = 0 \tag{84}$$

where

$$A = (1-s)\left[1+\delta+\frac{1}{\kappa}(1+\alpha)\right]$$

$$B = 2\frac{G^*}{G_t}+\frac{1}{\kappa}(1+\alpha s)-(1+\delta s)$$

$$C = (1+s)\left[(1-\delta)+\frac{1}{\kappa}(1-\alpha)\right]$$

$$P = (1-s)\left[\left(1-\delta-\frac{1}{\kappa}(1-\alpha)+\frac{1}{\kappa}(1-\alpha\delta)(\sigma+s)\frac{G_t}{G^*}\right)\right] \tag{85}$$

$$Q = (1-\sigma)\left[1-\delta+\frac{1}{\kappa}(1-\alpha)\right]$$

$$R = 4\frac{G^*}{G_t}+(1+s)\left[\frac{1}{\kappa}(1+\alpha)-(1+\delta)\right]-(\sigma-s)\left[1-\delta-\frac{1}{\kappa}(1+\alpha)\right.$$
$$\left.+\frac{1}{\kappa}(1-\alpha\delta)(1+s)\frac{G_t}{G^*}\right]$$

with

$$\sigma = \frac{\sigma_{xx}+\sigma_{yy}}{2G_t}$$

Criteria (83) and (84) have been evaluated numerically for the plane strain compression path with the Castlegate sandstone and Jurassic shale data. The results are shown in Figures 1 and 2 for flow and deformation theory versions of the MC and DP models. From these findings it may concluded that surface instabilities occur well ahead of the ellipticity limit. Also, deformation theory predictions are much below those obtained from flow theory—in common with earlier studies in metal plasticity.[7,8] In fact, flow theory results for failure of ellipticity and for onset of surface instabilities are at unrealistically high levels of strain (Figure 1). These observations should be helpful in constructing appropriate constitutive relations for elastoplastic response of pressure sensitive geometrials. The inadequacy of flow theory in explaining the experimental results on shear band formation in sand has been recently suggested by Papamichos and Vardoulakis.[24]

We have also examined the influence of non-associativity on incremental response in the plastic range. Using the power law (78) with $\bar{K} = 10^{-7}$, $\bar{Y} = 25$ MPa, $n = 3{\cdot}5$, $\bar{\mu} = 3$, $E = 10^4$ MPa and $\nu = 0{\cdot}3$, the primary plane-strain compression curves are traced in Figure 5 for three different values of $\bar{\eta}$. Calculations were made with flow theories of MC and DP inner cone models (material parameters for DP inner cone are evaluated from (80)) but deformation theories result in almost the same behaviour. Note that here $\sigma_1 = 0$ so that $\bar{\sigma}_e = \bar{\phi} = -\sigma_3$ and the MC curve in Figure 5 is independent of $\bar{\eta}$ (and identical for flow and deformation theories). The DP inner cone response shows stiffer behaviour with increasing $\bar{\eta}$.

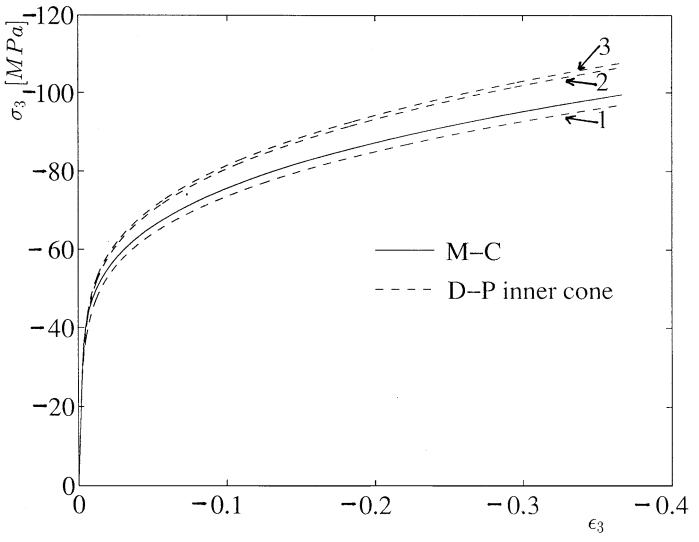

Figure 5. Stress–strain response in plane-strain axial compression for a power-law material at different levels of non-assiciativity. For all curves $\bar{\mu} = 3$ and values of $\bar{\eta}$ are indicated near the appropriate curves. Notice that for this particular loading path MC results do not depend on $\bar{\eta}$

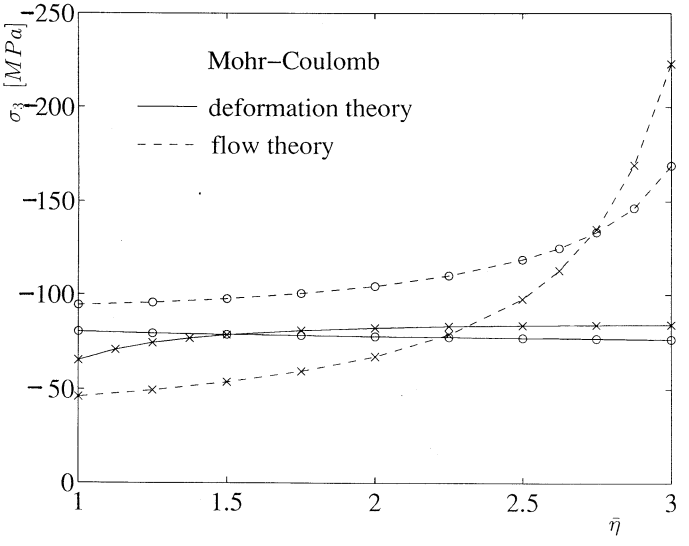

Figure 6. Onset of surface instabilities, indicated by (o), and loss of ellipticity, indicated by (x), at different levels of non-associativity. Results are for Mohr–Coulomb models with a fixed value of $\bar{\mu} = 3$

Onset of surface instabilities and failure of ellipticity at different levels of non-associativity is shown in Figures 6 and 7 for the plane-strain compression response of Figure 5. Here $\bar{\mu}$ has been kept constant ($= 3$) with $\bar{\eta}$ varying in the range 1–3. It is apparent that the flow theory predictions are very sensitive to deviations from associativity. At sufficiently low values of $\bar{\eta}$ flow theory

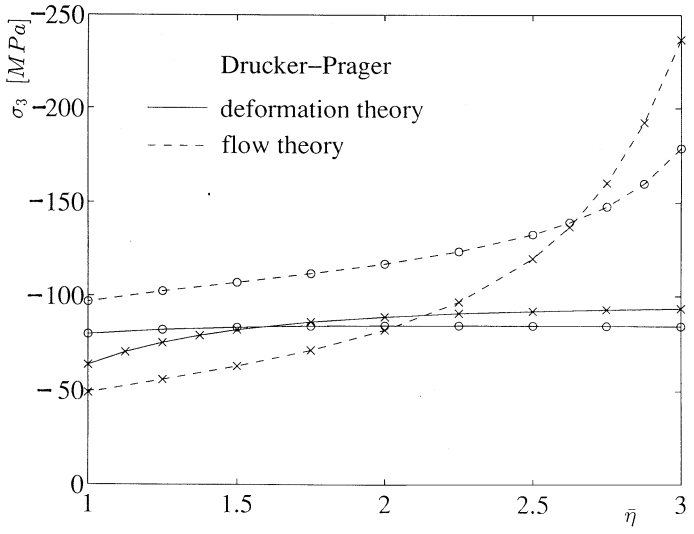

Figure 7. Onset of surface instabilities, indicated by (o), and loss of ellipticity, indicated by (x), at different levels of non-associativity. Results are for Drucker–Prager models with a fixed value of $\bar{\mu} = 3$

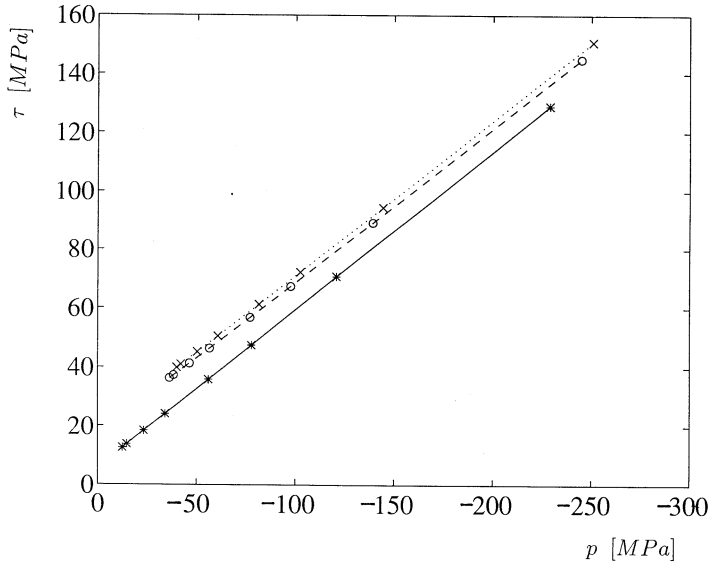

Figure 8. Initial yield ($*$), onset of surface instabilities (o) and loss of ellipticity (x), at different levels of confining pressure in plane-strain compression. Results are for Castlegate sandstone with Mohr–Coulomb deformation theory. Here $p = (\sigma_1 + \sigma_3)/2$ and $\tau = (\sigma_1 - \sigma_3)/2$

predicts (for both models) failure of ellipticity before the occurrence of surface instabilities. This particular feature of flow theory can facilitate the modelling of possible emergence of shear bands and fracture in plane strain compression test. Flow theory stress results for loss of ellipticity may

become even smaller than those of deformation theory (Figures 6 and 7). The latter model, by constrast, shows little sensitivity to material non-associativity.

Our final figure (Figure 8) shows the predicted effect of confining pressure σ_1 on the behaviour of Castlegate sandstone in plane-strain compression. Loci on initial yield, onset of surface instability and loss of ellipticity are plotted in the ($p = (\sigma_1 + \sigma_3)/2$, $\tau = (\sigma_1 - \sigma_3)/2$) plane, for different values of confining pressure, using the MC deformation theory. Since the surface instabilities and loss of ellipticity loci appear to be almost straight lines, which are nearly parallel to the initial yield line, it is worth asking whether the onset of surface instabilities and loss of ellipticity occur at definite values of effective stress. Work is now in progress in an attempt to address this issue. A more detailed analysis of the emergence of localized strain regions should account for a complete boundary value problem, along the lines followed by Papanastasiou[12] for elastoplastic solids and recently suggested by Ogden and Connor[25] for hyperelastic solids.

6. CONCLUSIONS

In this paper we derived constitutive relations for large strain elastoplastic response of pressure sensitive geomaterials. Tensorially invariant formulations of the Mohr–Coulomb and Ducker–Prager models, with arbitrary hardening and non-associated response are presented. In the absence of pressure sensitivity we recover from our formulation the large strain Tresca and von Mises models suitable for metal plasticity. Both flow and deformation theories were constructed, leading to linear incremental relations between the Eulerian strain rate tensor and the objective Jaumann stress rate tensor. The analysis was supplemented with criteria for detecting bifurcation points during loading history.

Specifying the constitutive relations for plane strain compression we show that deformation theory produces a much smaller instantaneous tangent shear modulus than flow theory. This is true for both MC and DP models. It follows that failure of ellipticity and onset of surface instabilities along the primary path, predicted by deformation theory for associated solids occur at much lower levels of strain than the corresponding flow theory results. However, flow theory predictions admit a considerable sensitivity to the level of non-associativity. In fact, at high levels of non-associativity flow theory predictions for loss of ellipticity can be at load levels below those obtained from deformation theory. More work is required to enable a reliable assessment of flow and deformation theory predictions, covering a range of material properties and non-orthogonal deformation patterns.

ACKNOWLEDGEMENT

The authors wish to thank Schlumberger for giving permission to publish this work. Part of this study was supported by the fund for promotion of research at the Technion.

REFERENCES

1. J. W. Rudnicki and J. R. Rice, 'Conditions for the localization of the deformation in pressure sensitive dilatant materials', *J. Mech. Phys. Solids*, **23,** 371–394 (1995).
2. I. Vardoulakis, 'Bifurcation analysis of the plane rectilinear deformation on dry sand samples', *Int. j. solids struct.*, **17,** 1085–1101 (1981).
3. K.-T. Chau and J. W. Rudnicki, 'Bifurcations of compressible pressure sensitive materials in plane strain tension and compression', *J. Mech. Phys. Solids*, **38,** 875–898 (1990).

4. D. R. J. Owen and E. Hinton, *Finite Elements in Plasticity*, Pineridge Press, Swansea, 1980.
5. C. S. Desai and H. J. Siriwardane, *Constitutive Laws for Engineering Materials*, Prentice-Hall, Englewood Cliffs, NJ, 1984.
6. W. F. Chen and D. J. Han, *Plasticity for Structural Engineers*, Springer, New York, 1988.
7. J. L. Bassani, D. Durban and J. W. Hutchinson, 'Bifurcation at a spherical hole in an infinite elastoplastic medium', *Math. Proc. Camb. Phil. Soc.*, **87,** 339–356 (1980).
8. E. Ore and D. Durban, 'Elastoplastic buckling of annular plates in pure shear', *J. Appl. Mech.*, **56,** 644–651 (1989).
9. I. Vardoulakis and P. Papanastasiou,' Bifurcation analysis of deep boreholes: I. Surface Instabilities', *Int. j. numer anal. methods geomech.*, **12,** 379–399 (1988).
10. P. Papanastasiou and I. Vardoulakis, 'Bifurcation analysis of deep boreholes: II Scale effect', *Int. j. numer. anal. methods geomech.*, **13,** 183–198 (1989).
11. P. Papanastasiou and I. Vardoulakis, 'Numerical treatment of progressive localization in relation to borehole stability', *Int. j. numer. anal. methods geomech.*, **16,** 389–324 (1992).
12. P. Papanastasiou, 'Numerical Analysis of Localization Phenomena with Application in Deep Boreholes', *Ph. D thesis*, University of Minnesota, 1990.
13. K.-T. Chau, 'Non-normality and bifurcation in a compressible pressure-sensitive circular cylinder under axisymmetric tension and compression', *Int. j. solids struct.*, **29,** 801–824 (1992).
14. R. Chambon, J. Desrues, W. Hammad and R. Charlier, 'CLoE, a new rate-type constitutive model for geomaterials theoretical basis and implementation', *Int. j. numer. anal. methods geomech.*, **18,** 253–278, (1994).
15. D. Durban, 'On the differentiation of tensor functions', *Math. Proc. Comb. Phil. Soc.*, **83,** 289–297 (1978).
16. D. Durban and M. Baruch, 'Natural stress rate', *Quart. Appl. Math.*, **35,** 55–61 (1977).
17. D. Durban and M. Kubi, 'A general solution for the pressurized elastoplastic tube', *J. appl. mech.*, **59,** 20–26 (1992).
18. R. W. Ogden, *Non-linear Elastic Deformations*, Ellis Horwood 1984.
19. R. Hill, 'Aspects of invariance in solid mechanics', in *Advances in Applied Mechanics*, vol. 18, Academic Press, New York, 1978, pp. 1–75.
20. D. Durban, 'A comparative study of simple shear at finite strains of elastoplastic solids', *Quart. J. Mech. Appl. Math.*, **43,** 449–465 (1990).
21. D. Durban and N. A. Fleck, 'Spherical cavity expansion in a Drucker-Prager solid', *J. Appl. Mech.*, 1997, to appear.
22. P. Papanastasiou and D. Durban, 'Elastoplastic analysis of cylindrical cavity problems in geomaterials', *Int. j. numer. anal. methods geomech.*, **21,** 133–149 (1997).
23. W. A. Olsson, 'Development of anisotropy in the incremental shear moduli for rock undergoing inelastic deformation', *Mech. Mater.*, **21,** 231–242 (1995).
24. E. Papamichos and I. Vardoulakis, 'Shear band formation in sand according to non-coaxial plasticity model', *Geotechnique*, **45,** 649–661, (1995).
25. R. W. Ogden and P. Connor, 'On the stability of shear bands', in D. F. Parker and A. H. England (eds), *IUTAM Symp. on Anisotropy, Inhomogeneity and Nonlinearity in Solid Mechanics*, Kluwer academic Publisher (1995), pp. 217–222.

